J. Phys. C: Solid State Phys., 17 (1984) 6781–6791. Printed in Great Britain

j–B characteristics of S-type in the presence of multivalued electron distribution between the equivalent valleys in Si

M Asche†, H Kostial†, V M Ivastchenko‡ and V V Mitin‡

† Zentralinstitut für Elektronenphysik der AdW der DDR, Mohren strasse 40/41, 1080, Berlin, GDR

‡ Institute of Semiconductors of the Ukrainian Academy of Sciences pr. Nauki 115, 252028, Kiev, USSR

Received 24 October 1983, in final form 26 March 1984

Abstract. In n-Si the dependence of the current density j and the transverse electric field $E_\perp$ on the applied electric field strength E_x is investigated theoretically and experimentally in the presence of a magnetic induction B perpendicular to the current, which can lead to a multivalued electron distribution between the valleys (MED) because the total field E (not only E_x) heats the carriers (this is related to the fact that partial transverse currents of electrons in different valleys exist regardless of the absence of the transverse current). For a homogeneous distribution of j and E numerical calculations deliver S-type j–B characteristics in the region of MED, which in turn, on account of the instability of a state with negative $\mathrm{d}j/\mathrm{d}B$, leads to an inhomogeneous current distribution. A layer of high current density, in which the electrons are repopulated into the valleys with high mobility along E_x, is built up near one side of the sample. With increasing B the wall parallel to the current between the layers with high and low current density quickly moves to the opposite surface. This is accompanied by a jump-like change of the transverse field and a strong increase of the current.

1. Introduction

In the papers of Asche *et al* (1980, 1981a, b) the multivalued electron distribution (MED) in n-Si at 27 K was investigated in detail for the case of the total current density j_x chosen along [110]. Instead of an equal carrier heating and distribution between the two valleys 1 and 2, situated symmetrically with respect to j_x (see figure 1*a*), in the region of E_x between 40 and 200 V cm^{-1} one of the valleys is populated predominantly. We shall now repeat the description of this phenomena presented by Gribnikov *et al* (1970) and Asche *et al* (1981a, b).

In the heating electric field where this phenomena is observed, electrons of valley 3 are hottest, so this valley is empty. For the explanation of MED let us consider a two-valley semiconductor which is bounded in the direction of the y axis (figure 1*b*). An external electric field E_x is applied along the x axis and j_x is the corresponding current. This current has two identical components:

$$j_x^{(1)} = j_x^{(2)} \qquad j_x^{(1,2)} = en_{1,2}\mu_{xx}^{(1,2)}E_x \qquad n_1 = n_2 \qquad \mu_{xx}^{(1)} = \mu_{xx}^{(2)}$$

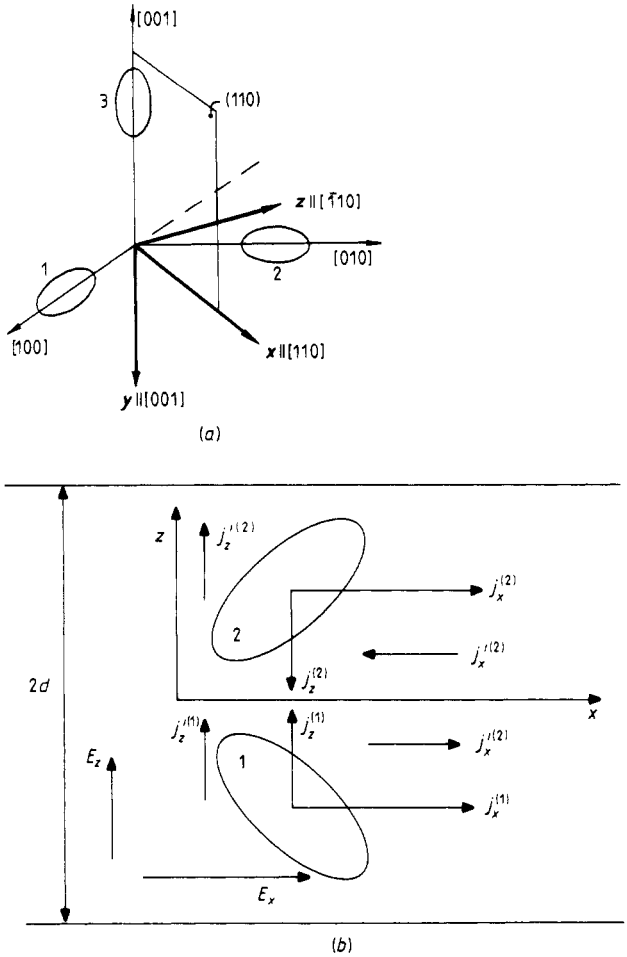

Figure 1. (*a*) Orientation of axes x, y, z and of valleys in Si. (*b*) Fields and partial currents in a two-valley semiconductor.

due to electrons from different valleys. Moreover, electrons from valleys 1 and 2 carry equal but oppositely directed currents:

$$j_z^{(1)} = -j_z^{(2)} \qquad j_z^{(1,2)} = en_{1,2}\mu_{zx}^{(1,2)}E_x \qquad \mu_{zx}^{(2)} = -\mu_{zx}^{(1)}$$

so that the total current is $j_z = 0$.

Let us assume that in addition to the field E_x there is also a weak fluctuation field E_z. This field can alter the average electron energy. Firstly, it cools electrons from the valley 2 and heats electrons from the valley 1 at the cost of powers $E_z j_z^{(2)}$ and $E_z j_z^{(1)}$, as shown in figure 1(*b*); secondly, the fluctuation field alters the heating by the field E_x: electrons from the valley 2 are cooled slightly by the power $E_x j_x'^{(2)}$ (a prime denotes the components of the current due to the fluctuation field E_z: $j_x'^{(1,2)} = en_{1,2}\mu_{xz}^{(1,2)}E_z$), and the electrons from the valley 1 are heated by the power $E_x j_x'^{(1)}$; thirdly, the field E_z heats to the same extent the electrons in both valleys at the expense of the powers $E_z j_z'^{(1)}$ and $E_z j_z'^{(2)}$ (this is an effect of the second order of smallness because $j_z'^{(1,2)} = en_{1,2}\mu_{zz}^{(1,2)}E_z$).

For the first two reasons the electrons in the first valley are heated more strongly than those in the second valley. If the intervalley transition time decreases with an increase of the energy of the electrons, they are transferred from the first valley to the second, so that the conductivity becomes anisotropic. For simplicity it is assumed that the electron mobility is not strongly dependent on the heating, which is in agreement with the available data for Ge and Si, i.e. it is assumed that even if the heating of the valleys is different, still $\mu_{xx}^{(1)} \approx \mu_{xx}^{(2)}$, $\mu_{zz}^{(1)} \approx \mu_{zz}^{(2)}$ and $\mu_{xz}^{(2)} \approx -\mu_{xz}^{(1)}$. Then there is little change in the current components j_x and j_z' but new components j_z and j_x' appear and these are due to the non-diagonal components of the conductivity tensor directed (figure 1*a*) opposite to j_z' and j_x.

If the transfer of electrons from the hot to the cold valley does not depend strongly on the heating field, so that $|j_z| < |j_z'|$, fluctuations of the field E_z die out and there are no special effects. However, if the electron density in the hot valley decreases strongly on increase in the heating field, then at some critical field E_c the current $|j_z|$ can exceed $|j_z'|$. The fluctuation field E_z grows and a new non-equilibrium anisotropic state appears in the semiconductor in which the second valley is predominantly populated and a finite transverse electric field is established.

Similarly, it is possible to consider a fluctuation E_z of the opposite sign, which, subject to the condition $|j_z| > |j_z'|$, gives rise to an anisotropic state in which the first valley is predominantly populated, i.e. the MED effect arises.

As theoretically shown in the paper of Asche *et al* (1983) for the current chosen in a (001) plane MED can be realised for directions of j_x departing less than 15° from [110]. For these orientations, besides the state with a dominating population of that valley, in which the carriers are less heated on account of the chosen departure of j_x from the symmetry axis, the creation of a transverse field permits a state with a preponderent population of the other valley too. The electrons of the third valley are more strongly heated than the others and are therefore transferred to the other valleys.

If the x axis is chosen in the $(\bar{1}10)$ plane its departure from [110] leaves the symmetry of the valleys 1 and 2 unchanged (see figure 1*a*) and MED between the two valleys can be realised for j_x declining from [110] up to 36° (i.e. up to [111] direction). For greater departures MED cannot be realised, because the electrons become transferred from both valleys 1 and 2 into valley 3.

As shown in work of Mitin (1971) (see also § 22 in the book of Asche *et al* (1982)) in many-valley semiconductors for each current direction a magnetic field can be applied in the plane transverse to j_x in such a direction and with such a field strength that the carriers of two valleys become equally heated. However, in the paper of Mitin (1971) only high temperatures were considered, for which MED cannot be realised. In the present paper MED is investigated in detail in the presence of B for such current orientations, which do not exhibit MED in the absence of B, and it is shown that as a consequence of MED S-type j–B characteristics as well as an S-type dependence of the transverse electric field on the magnetic induction B is realised.

2. Theoretical considerations

In accordance with Mitin (1971) a two-valley semiconductor is considered when the current orientation x declines from the symmetry axis by an angle φ into the direction of the main axis of valley 2 and the transverse magnetic induction B is chosen along the y axis (see figure 1*b*). On account of symmetry it is sufficient to investigate $0 \leqslant \varphi \leqslant \pi/4$.

As usual the transverse electric field component $E_z = \vartheta E_x$ created in the sample is determined by the condition that the transverse current vanishes:

$$\nu = -\frac{BF_1 + aF\cos 2\varphi}{1 - aF\sin 2\varphi} \tag{1}$$

with

$$F = \frac{\phi_1 - \phi_2}{\phi_1 + \phi_2} \qquad F_1 = \frac{\psi_1 + \psi_2}{\phi_1 + \phi_2} \qquad a = \frac{\mu_\perp - \mu_\parallel}{\mu_\perp + \mu_\parallel} \qquad \phi_\alpha = \mu_\alpha \tau_\alpha \qquad \psi_\alpha = \tilde{\mu}_\alpha \tau_\alpha \tag{2}$$

and $\tau_\alpha = \tau(E_\alpha)$ for the out-scattering time from valley α ($\alpha = 1, 2$) into valley β ($\beta = 2, 1$), $\mu_\alpha = \mu(E_\alpha)$ and $\tilde{\mu}_\alpha B = \tilde{\mu}(E_\alpha)B$ are mobilities dependent on the effective field strength E_α in the valley α and we denote

$$\begin{aligned} \mu_\alpha &= \tfrac{1}{2}(\mu_\parallel^{(\alpha)} + \mu_\perp^{(\alpha)}) \\ \mu_{\parallel,\perp}^{(\alpha)} &= \tfrac{2}{3}e\int_0^\infty \frac{\varepsilon g(\varepsilon)(\tau/m)_{\parallel,\perp}}{1 + (\tau/m)_\parallel(\tau/m)_\perp(eB/c)^2}\left(-\frac{\partial F_0^{(\alpha)}}{\partial \varepsilon}\right)\mathrm{d}\varepsilon \\ \tilde{\mu}_\alpha &= \frac{2}{3}\frac{e^2}{c}\int_0^\infty \frac{\varepsilon g(\varepsilon)(\tau/m)_\parallel(\tau/m)_\perp}{1 + (\tau/m)_\parallel(\tau/m)_\perp(eB/c)^2}\left(-\frac{\partial F_0^{(\alpha)}}{\partial \varepsilon}\right)\mathrm{d}\varepsilon \end{aligned} \tag{3}$$

with e for the electron charge and c for the velocity of light; $\tau_{\parallel,\perp}$ are the parallel and perpendicular tensor components for the momentum relaxation time depending on the carrier energy; $m_{\parallel,\perp}$ are the respective components of the effective-mass tensor; the parallel axis coincides with the axis of rotation of the ellipsoid of the surface of constant energy; $F_0^{(\alpha)}$ is the symmetric part of the distribution function in valley α and $g(\varepsilon)$ is the density of states. Equation (1) was obtained assuming that for each magnetic field strength an effective electric field with respect to the valley α can be defined (see Appendix)

$$E_{1,2} = E_x[1 \pm a\sin 2\varphi \pm 2a\vartheta\cos 2\varphi + (1 \mp a\sin 2\varphi)\vartheta^2]^{1/2} \tag{4}$$

which completely determines the values of the functions† $\tau_\alpha = \tau(E_\alpha)$, $\mu_\alpha = \mu(E_\alpha)$, $\tilde{\mu}_\alpha = \tilde{\mu}(E_\alpha)$. Because E_α and F depend on ϑ, equation (1) is non-linear with respect to ϑ and in a certain region of E_x and B it can exhibit more than one solution, i.e. MED can be realised.

Further on we determine the conditions for MED. It is necessary that in the absence of MED the electrons of both valleys are almost equally heated. For each current direction φ, from equation (4) two values of ϑ can be obtained, for which $E_1 = E_2$:

$$\vartheta_1 = -\frac{1 + \cos 2\varphi}{\sin 2\varphi} \qquad \vartheta_2 = -\frac{1 - \cos 2\varphi}{\sin 2\varphi}. \tag{5}$$

On inserting either ϑ_1 or ϑ_2 into equation (1) consequently two values B_1 or B_2 connected with equal carrier heating in both valleys result:

$$B_1 = -\frac{1}{F_1(B_1)}\frac{1 + \cos 2\varphi}{\sin 2\varphi} < 0 \qquad B_2 = \frac{1}{F_1(B_2)}\frac{1 - \cos 2\varphi}{\sin 2\varphi} > 0. \tag{6}$$

† Bearing in mind that $\tau(E_\alpha)$ changes with E_α in a more pronounced way than $\mu(E_\alpha)$ and $\tilde{\mu}(E_\alpha)$, in the present section (however, not in § 3) we shall assume μ_α and $\tilde{\mu}_\alpha$ to be independent of E_α. In this approximation F_1, too, does not depend on E_α and changes weakly with increasing B, and F reduces to $(\tau_1 - \tau_2)/(\tau_1 + \tau_2) = (n_1 - n_2)/(n_1 + n_2)$ characterising the intervalley redistribution of electrons with n_α denoting the carrier concentration in valley α.

It should be noticed that the critical values of B do not depend on E_x in the present approximation which neglects the dependence of μ_α and $\bar{\mu}_\alpha$ on E_α.

The condition for MED can be obtained by investigating the solution of equation (1) in the neighbourhood of the state with equal carrier heating in both valleys. Inserting either of B_i into equation (1), one obtains

$$\vartheta = \frac{\vartheta_i - aF\cos 2\varphi}{1 - aF\sin 2\varphi}. \tag{7}$$

Equations (7) and (4) can be developed with respect to the small departure of ϑ from ϑ_i and in an analogous way to Gribnikov *et al* (1970) they deliver that for

$$-a^2 \frac{\mathrm{d}\ln \tau_\alpha}{\mathrm{d}\ln E_\alpha}\bigg|_{E_\alpha = E_\alpha(\vartheta_{1,2})} \frac{1}{1+\vartheta_{1,2}^2} > 0 \tag{8}$$

there are three solutions of equation (1), i.e. MED is realised, but for the case inverse to (8) the solution is unique. The criterion (8) differs from the one investigated in detail for the absence of B in the paper of Gribnikov *et al* (1970) by the factor $(1+\vartheta_i^2)^{-1}$ on the left-hand side and by the condition that $\tau(E)$ has to be evaluated for the values of B_i considered.

Figure 2 shows the dependence of F, ϑ and j_x on B in the neighbourhood of B_2 for E_α chosen in the region of E_x and B where the inequality (8) is fulfilled. In correspondence to the three solutions for ϑ in the neighbourhood of B_2, there are three different electron distributions between the valleys: $F > 0$ and $F < 0$ describe the predominant population of valleys 1 and 2, respectively, while $F = 0$ is of course related to the equal electron distribution. The three different electron distributions between the valleys lead to three different current densities. In the neighbourhood of B_2 the dependence of j_x on B exhibits an S-type region if $\varphi > \tan^{-1} a$, as shown by curve 3 in figure 2, while near B_1 the j–B characteristics are always of S-type as can be seen (compare with Mitin (1971)) from

$$j_x = -n\mu E_x[1 + (BF_1)^2]\left(1 - \frac{a^2F^2}{1+(BF_1)^2}\right)(1 - aF\sin 2\varphi)^{-1}. \tag{9}$$

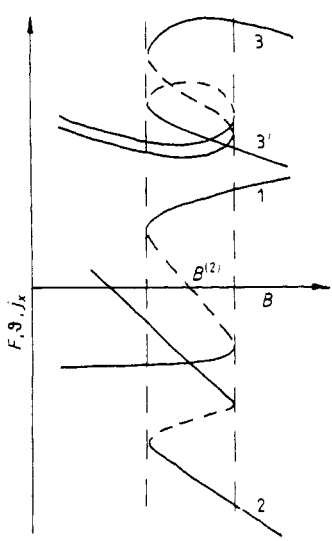

Figure 2. Dependences of F (curve 1), ϑ (curve 2) and j_x (curve 3 for $\varphi > \tan^{-1} a$ and 3′ for $\varphi < \tan^{-1} a$) on the magnetic induction B.

By the way, in Gribnikov *et al* (1970) it had been demonstrated that in the absence of B MED is possible if $\varphi < \tan^{-1} a$. For such an orientation $j_x(B)$ in the neighbourhood of B_2 behaves as shown by curve 3′. With decreasing φ the loop shown in the characteristics 3′ grows while according to equation (6) the value of B_2 decreases. In the limit $\varphi \to 0$ the values of B_2 and B_1 become 0 and ∞, respectively. With increasing φ the loop diminishes and it vanishes for $\varphi \simeq \tan^{-1} a$, while the S-type behaviour becomes possible as mentioned above.

3. Results

Measurements of j_x as well as the transverse field E_- versus B and E_x were performed at 27 K (liquid neon temperature) for samples of n-Si with a small concentration of acceptors (Asche *et al* 1981a, b). The brick-shaped samples were cut from a $(\bar{1}10)$ plate with the direction of the current departing from [110] by $\varphi = 53°$. A magnetic induction B was applied in the yz plane perpendicular to the current j_x, and the axis z was directed along $[\bar{1}10]$ as in figure 1(a). Monte Carlo calculations were performed for the same case in the approximation of weak magnetic fields and the dependence of μ_α, $\bar{\mu}_\alpha$ and τ_α on E and B were taken into account. Here the impurity intervalley scattering time is chosen to be 10^{-7} s. We used the same method of calculation and constant as Asche *et al* (1981b) and Ivastchenko and Mitin (1984). That is why we only want to note here that for electric fields of 40 to 150 V cm^{-1}, where the effect of interest takes place, the mean energy of the electrons is then 3 to 7 times larger than for equilibrium conditions ($T = 27$ K). Monte Carlo calculations give high accuracy as normal for strong-heating electric fields. The introduction of B changes only the equation of motion of the electrons between collisions and in addition to the case of $B = 0$ it is necessary to calculate additional components of the current.

Figures 3(a) and (b) present the experimental and numerical results for $j_x(B_z)$. If the applied electric field is chosen between 60 and 150 V cm^{-1} for $B > 0$ the experimental results show a strong increase of the current in a small region of magnetic field strength. For this region of applied electric fields the numerical calculations deliver an S-type behaviour of $j_x(B_z)$† on account of MED‡. It can be shown that the part of the characteristics with $\mathrm{d}j_x/\mathrm{d}B_z < 0$ is unstable (in figure 3(b) and further on the unstable parts are depicted by broken curves). In order to obtain the experimentally observable characteristics for this case it is necessary (Mitin 1977) to determine the dependence of the transverse field E_y on y using the continuity equation for the current densities of each valley. (The dependence of E_y on B, which is necessary for these calculations, is shown in figure 3(c). This dependence also exhibits an S-type behaviour for electric fields applied within the region with MED.)

There are two stable solutions, each connected with certain boundary conditions on the surfaces $y = -d$ and $y = +d$, as shown in figures 3(b) and (c) by curves A and B. In

† To obtain the current j_x from the theoretical results it is necessary to multiply the mean drift velocity of electrons $v_d(E)$ by their charge e and density n.

‡ The multivalued electron distribution described in the present section is analogous to the effect for the two-valley model discussed in the preceding section, because the valleys 1 and 2 are equivalent and can be presented as one valley while the valley 3 plays the role of the second valley. However, for high magnetic fields—yet in a narrower region of E_x than discussed above—the equivalence of valleys 1 and 2 may be destroyed and MED can be realised between them. This effect leads to a decrease of the current, an increase of $E_y = \vartheta E_x$ as exhibited by the chain curve in figure 3(b), (c) and the appearance of an additional electrical field E_z.

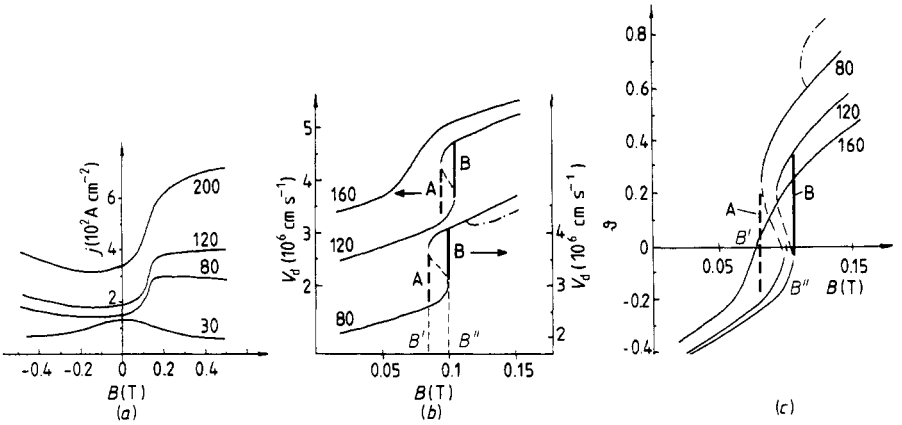

Figure 3. Dependence of the current density (*a*, *b*) and of $\vartheta = E_y/E_x$(*c*) on the magnetic induction for $B = B_z$ ((*a*)—experimental results, (*b*), (*c*)—numerical results) at various values of the applied average electric field strength E_x (in units of V cm^{-1} marked on the curves). $T = 27$ K.

the case of curve A at one of the surfaces considered a layer with high current density is built up when the magnetic induction reaches a critical value B' (for curve B such a behaviour is obtained for B''). The steep wall between the layers of high and low current density—it is situated parallel to the surfaces $y = \pm d$ if the transverse field has a y component only—shifts to the opposite surface on further increase in B. Comparing these numerical results with the experimental data, it can be concluded that case B is realised because there is a smooth rise of the current from its low values up to the critical magnetic field, for which it changes in a jump-like way. The experimental results show a less steep increase on account of the influence of the contacts, which shunt the transverse fields in their vicinity. Therefore the applied voltage is not distributed in a uniform way along the sample and this inhomogeneous distribution sensitively depends on the changes of E_y with B near B'' (or near B' in case A).

If the applied electric fields are already higher than the values of the region for which MED is realised, instead of S-type characteristics we obtain the type of dependence shown in figure 3(*b*) for $E_x = 160$ V cm^{-1}, which demonstrates a still strongly pronounced rise of the current in a narrow region of magnetic field strength. Such a behaviour is observed experimentally, too, as shown by the curve for $E_x = 200$ V cm^{-1} in figure 3(*a*). On the other hand, for weak electric fields applied (the curve for $E_x = 30$ V cm^{-1} in figure 3*a*) an influence of the magnetic field on the current density is seen as expected due to the usual magnetoconductivity.

For $B < 0$ the direction of the total electric field shifts with increasing magnetic field towards ⟨001⟩ and further on towards ⟨111⟩ and the dominant population of the third valley therefore vanishes for strong B and the current begins to rise (figure 3*a*) in agreement with the calculations because for $\varphi < 60°$ MED is not observed for $B < 0$.

In figure 4 the calculated j_x–E_x behaviour is demonstrated for several values of B; the unstable parts of the characteristics are presented by broken lines as mentioned above. In the absence of B on account of the long-time measurements, of course, instead of n-type characteristics current saturation is observed due to domainisation, as shown by the thick full curve for $j = j_{max}$ for the case realised experimentally in contrast to $j = j_{min}$

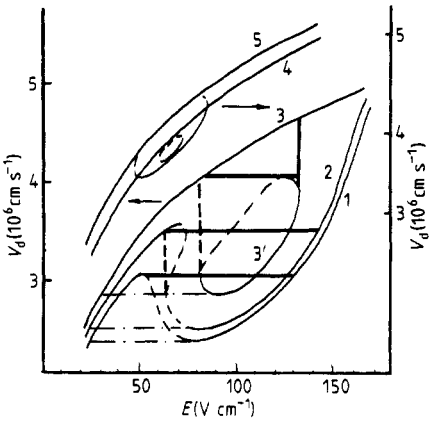

Figure 4. Dependence of V_d on the applied electric field E_x for various values of the magnetic field $B = B_z$: B = 0(1); 0.078 T(2); 0.3 (3, 3'); 0.11 (4) and 0.13 T (5). T = 27 K.

(Gribnikov *et al* 1981) indicated by the chain curve. With increasing B the n-type negative differential conductivity (NDC) is changed into N–S-type. In the region of electric field strengths with three current values for each E_x the solutions are connected with different possible degrees of carrier population in valley 3, the lowest value corresponding to the highest degree, of course. With increasing B, when the total electric field has already been turned near to ⟨111⟩ a solution with preponderent population of valley 3 splits in the form of a loop from the smooth curve, which represents the solution with overwhelming population of valleys 1 and 2 (curve 3'). The experiments deliver a continuous decrease of the region with current saturation with growing B and no jump-like transition from characteristics with saturation to one with smoothly increasing current at some certain magnetic field strength can be observed. This fact proves the existence of states which are connected with the lower branch of the loop. On increasing B further, the total electric field declines still more from ⟨111⟩ towards ⟨110⟩ and the loop realised on behalf of the preponderant population of the third valley vanishes. On the other hand MED between the valleys 1 and 2 appears (curve 4), but in another region of electric field strengths than the MED between valley 3 and valley 1 + 2 (see footnote ‡ on p. 6786). The MED between valleys 1 and 2 also leads to a loop in the beginning, which with on further increase of magnetic field joins the solution for a dominant but equal population of both valleys (curve 5). If the electric field were homogeneously distributed in the sample in the case of preponderant population of valley 3 the characteristics should show a behaviour as indicated by the thick broken curve (Gribnikov *et al* 1981). However, because this part of the characteristics is unstable the sample decays into domains with high and low field and the wall between them shifts with increasing applied electric field from the current contact to the other.

For other orientations of B, too, if the total field E can be directed symmetrically with respect to any two of the valleys, MED can be realised as discussed above with the only exception that the current direction does not lie in the plane that contains the main axes of the valleys considered. For instance, for B parallel to y (compare figure 1) when the total field E is turned away from E_x with increasing magnetic field MED becomes realised between the valleys 3 and 1 for $B > 0$ and between the valleys 3 and 2 for $B < 0$, respectively. In each case the third valley is depopulated. In figure 5(a) the dependence

of the component of the transverse electric field measured along y on B_y is shown for several values of the applied electric field, and figure 5(b) shows the calculated $E_y(B_y)$. Experimentally (curves for $E_x = 100\ \mathrm{V\,cm^{-1}}$ and $E_x = 200\ \mathrm{V\,cm^{-1}}$ in figure 5a) a sharp rise of E_y is observed for a certain value of the magnetic induction (compare description of figure 3) for those applied electric fields for which MED is realised between valleys 3 and 1 for $B > 0$ and valleys 3 and 2 for $B < 0$, respectively. The calculations deliver a multi-valued dependence, which is not observed, but a sharp rise of current density and transverse field as indicated by the thick lines in figure 5(b) is observed, because the

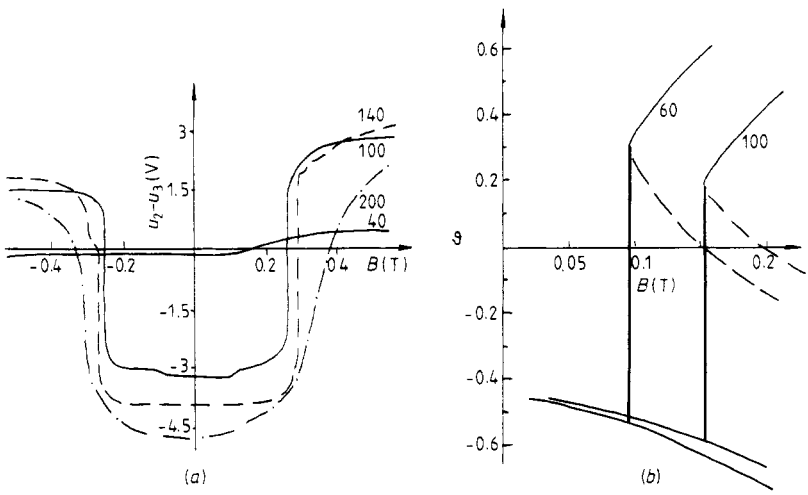

Figure 5. Dependence of transverse voltage $u_2 - u_3$ (a) and transverse electric field $\vartheta = E_y/E_x$(b) on the magnetic induction $B = B_y$ for various values of the applied average electric field strength E_x (in units of $\mathrm{V\,cm^{-1}}$ marked on the curves) at $T = 27$ K. (a) experimental values; (b) calculated values.

sample decays into layers of high and low current density, the electrons being distributed into valley 1 for $B > 0$ in the high-current-density layer and into valley 3 in the low-current-density layer. The difference of the values of B for the sharp rise obtained experimentally and theoretically is due to the fact that the weak magnetic field approximation is not valid for this case. For electric fields applied above the upper limit for MED a strongly pronounced rise of the transverse field remains (curve for $E_x = 200\ \mathrm{V\,cm^{-1}}$ in figure 5a) but it is no longer jump-like.

Figure 6 demonstrates the measured and calculated dependence of the current density on the angle ψ of the orientation of B in the plane perpendicular to j_x ($0 < \psi < 180$ with $\psi = 0$ denoting the direction of B along the z axis (figure 1a)). The current (figure 6a) changes significantly for those orientations, for which the numerical data (figure 6b) exhibit a change of the number of solutions.

The presented experimental and numerical data agree for applied electric fields above $80\ \mathrm{V\,cm^{-1}}$, i.e. when the high-electric-field domain has already covered the whole sample and E_x is distributed homogeneously therefore, while in the E_x region characterised by current saturation the applied field is inhomogeneous along the sample and the build-up of a layered structure with respect to the current density has to be discussed separately.

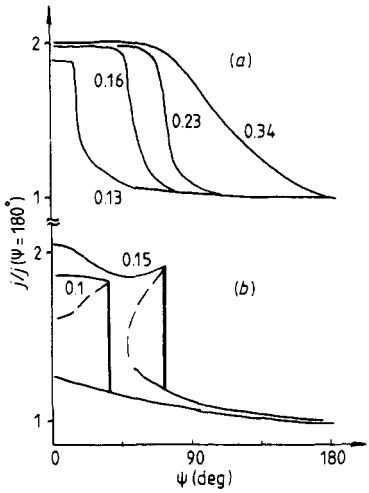

Figure 6. Ratio of the current densities $j_x(B(\psi))$ to $j_x(B(\psi = 180°))$ as a function of the orientation angle ψ of the magnetic induction B for an applied average electric field strength $E_x = 120\ \mathrm{V\,cm^{-1}}$ and different values of B (in units of T marked on the curves). $T = 27$ K. (*a*) experimental values; (*b*) calculated values.

Acknowledgments

The authors want to express their gratitude to Dr Z S Gribnikov for many useful discussions of the results.

Appendix

If the intervalley scattering time is considerably longer than all the intravalley scattering times, the transport equations for electrons from different valleys

$$-e[E_i + (1/c)(\boldsymbol{v} \times \boldsymbol{H})_i]\, \partial F_p^{(\alpha)}/\partial p_i = \hat{I} F_p^{(\alpha)} \tag{A1}$$

differ only in the field terms. Here $F_p^{(\alpha)}$ distribution function of electrons in valley α, $\boldsymbol{v} = \mathrm{d}\varepsilon/\mathrm{d}\boldsymbol{p}$ is the electron velocity, $\hat{I}$ is the operator of intra-valley scattering.

In the quasielastic approximation, we obtain $F_p^{(\alpha)} = F_p^{+(\alpha)} + F_p^{-(\alpha)} \cong F_0^{(\alpha)} + v_i F_i^{(\alpha)}$, $F^{+(\alpha)} \gg F^{-(\alpha)}$ are, respectively, the even and the odd parts (with respect to the momentum) of the distribution function. Introducing the momentum relaxation time tensor and assuming that $\boldsymbol{E} \perp \boldsymbol{B}$, we obtain in the system of the principal axes of the ellipsoid of the surface of the constant energy the following expression:

$$F_i^{(\alpha)} = e\left[\frac{\partial F_0}{\partial \varepsilon_p}\tau_{ii}\frac{E_i + \delta_{ikj}(e/c)E_k(\tau/m)_{kk}B_j}{1 + (e/c)^2(\tau/m)_\perp[B_1^2(\tau/m)_\perp + (B_2^2 + B_3^2)(\tau/m)_\parallel]}\right]^{(\alpha)}. \tag{A2}$$

Here the axis 1 coincides with parallel axis (compare with explanations of equation (3)). Note that equations (3) follow from (A2) if the current is calculated.

The equation for $F_0^{(\alpha)}$ then has the form

$$-\tfrac{2}{3}e^2\frac{\partial}{\partial\varepsilon}\left[\frac{\Sigma_i E_i^2(\tau/m)_{ii}\,\varepsilon g(\varepsilon)\,\partial F_0/\partial\varepsilon}{1 + (e/c)^2(\tau/m)_\perp[B_1^2(\tau/m)_\perp + (B_2^2 + B_3^2)(\tau/m)_\parallel]}\right]^{(\alpha)} = \hat{I}F_0^{(\alpha)}, \tag{A3}$$

where

$$\hat{I}F_0^{(\alpha)} = \sum_p \hat{I}F^{-(\alpha)}\delta(\varepsilon - \varepsilon_p) \simeq \sum_p \hat{I}\delta(\varepsilon - \varepsilon_p)F_0^{(\alpha)}.$$

In the case considered, i.e. when B is parallel to the valley's symmetry y axis, the denominator in square brackets is not dependent on α and for $\tau_\parallel(\varepsilon)/\tau_\perp(\varepsilon)$ = constant (then $\tau_\parallel(\varepsilon)/\tau_\perp(\varepsilon) \equiv \mu_\parallel/\mu_\perp$ and a in equations (1) and (4) is the same constant), we obtain from equation (A3)

$$-\frac{2}{3}e^2\frac{\partial}{\partial\varepsilon}\left[\frac{\frac{1}{2}[(\tau/m)_\parallel + (\tau/m)_\perp]\,\varepsilon g(\varepsilon)\,\partial/\partial\varepsilon}{1 + (eB/c)^2(\tau/m)_\parallel(\tau/m)_\perp}\right]F_0^{(\alpha)}E_\alpha^2 = \hat{I}F_0^{(\alpha)}. \tag{A4}$$

Here E_α^2 are also given by equation (4), i.e. the transport equations in the first and in the second valleys differ only in the factor E_α^2. Consequently, for a given B, the quantity E_α determines completely the distribution function $F_0^{(\alpha)} = F_0(E_\alpha)$, and, therefore, all the transport coefficients (equation (2)).

If the magnetic field is small, i.e. if it is possible to neglect the term of order B^2 in comparison with 1 in the denominator of equation (A3), then without any restriction on the direction of B and on the number of valleys and their orientation as to E, it is possible to introduce an appropriate effective field E_α. The influence of the magnetic field in this case is taken into account by the linear term in B in equation (A2) and hence through the transverse component of the electric field it changes E_α and the heating of the electrons in the valley α.

References

Asche M, Gribnikov Z S, Ivastchenko V M, Kostial H and Mitin V V 1983 *Phys. Status Solidi* (b) **114** 429

Asche M, Gribnikov Z S, Ivastchenko V M, Kostial H, Mitin V V and Sarbey O G 1981a *Preprint Inst. Phys. Ukr. Akad. Sci. N4* Kiev

—— 1981b *Zh. Eksp. Teor. Fiz.* **81** 1347

Asche M, Gribnikov Z S, Mitin V V and Sarbey O G 1982 *Goryachie elektrony v mnogodolinikh poluprovodnikakh* (Kiev: Naukova dumka)

Asche M, Kostial H and Sarbey O G 1980 *J. Phys. C: Solid State Phys.* **13** L645

Gribnikov Z S 1982

Gribnikov Z S, Ivastchenko V M, Mitin V V and Sarbey O G 1981 *Preprint Inst. Phys. Ukr. Acad. Sci. N 8* Kiev

Gribnikov Z S, Kochelap V A and Mitin V V 1970 *Zh. Eksp. Teor. Fiz.* **59** 1828

Ivastchenko V M and Mitin V V 1984 *Ukr. Phys. Zh.* **29** 123

Mitin V V 1971 *Fiz. Tech. Poluprov.* **5** 1739

—— 1977 *Fiz. Tech. Poluprov.* **11** 1233